6.5 Natural Convection in Enclosures

Enclosures are finite spaces bounded by walls and filled with fluid. Natural convection in enclosures, also known as internal convection, takes place in rooms and buildings, furnaces, cooling towers, as well as electronic cooling systems. Internal natural convection is different from the cases of external convection, where a heated or cooled wall is in contact with the quiescent fluid and the boundary layer can be developed without any restriction. Internal convection usually cannot be treated using simple boundary layer theory because the entire fluid in the enclosure engages to the convection.

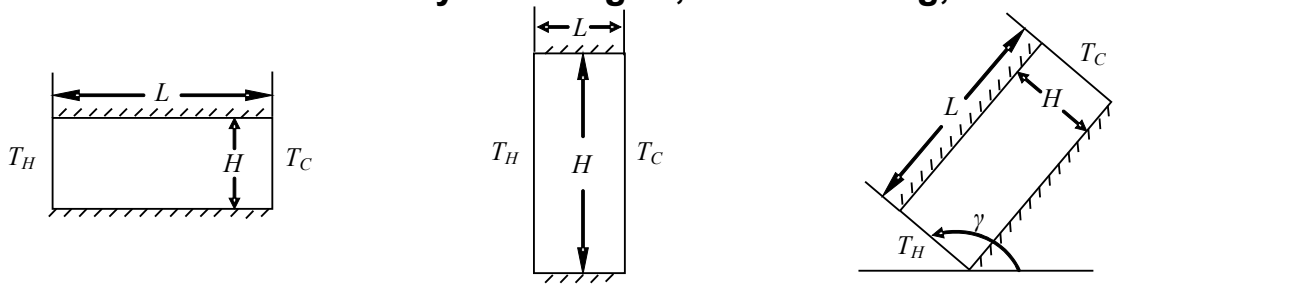

(a) shallow enclosure (b) tall enclosure (c) inclined enclosure

(d) enclosure with vertical partitions (e) concentric annulus

(f) box enclosure (g) truncated annular enclosure

(*b*)

Figure 6.17 Different configuration of natural convection in enclosures

6.5.1 Scale Analysis

- Two-dimensional natural convection in a rectangular enclosure with two differentially heated sides and insulated top and bottom surfaces (Fig. 6.18) will be considered.
- Assumed to be Newtonian and incompressible.
- Initially at a uniform temperature of zero.
- At time zero the two sides are instantaneously heated and cooled to $\Delta T/2$ and $-\Delta T/2$, respectively.
- The transient behavior of the system during the establishment of the natural convection is the subject of analysis

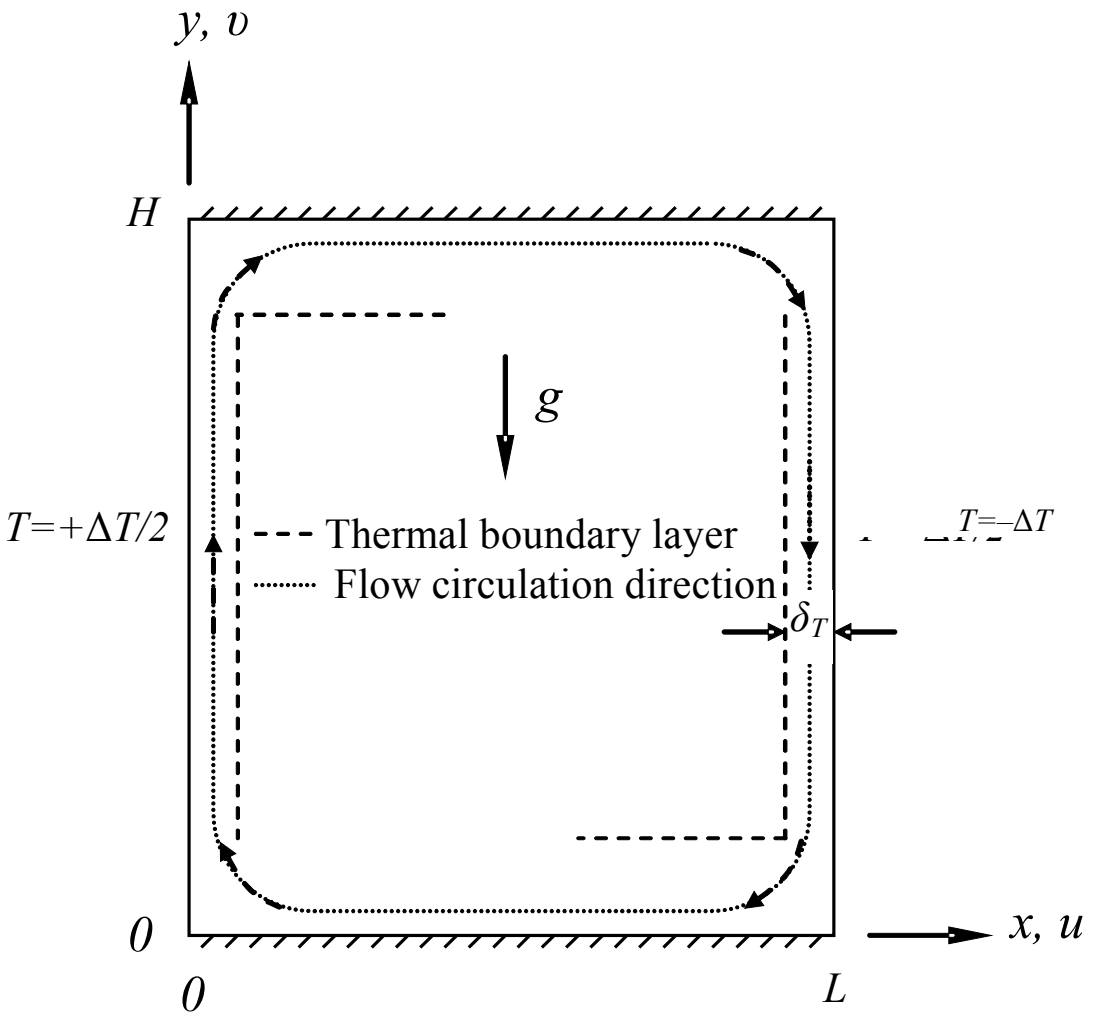

Figure 6.18 Two-dimensional natural convection in rectangular enclosure.

It is assumed that the fluid is single-component and that there is no internal heat generation in the fluid. Therefore, the governing equation for this internal convection problem can be obtained by simplifying eqs. (6.8), (6.13) and (6.14):

$$\frac{\partial u}{\partial x} + \frac{\partial v}{\partial y} = 0 \tag{6.205}$$

$$\frac{\partial u}{\partial t} + u\frac{\partial u}{\partial x} + v\frac{\partial u}{\partial y} = -\frac{1}{\rho}\frac{\partial p}{\partial x} + \nu\left(\frac{\partial^2 u}{\partial x^2} + \frac{\partial^2 u}{\partial y^2}\right) \tag{6.206}$$

$$\frac{\partial v}{\partial t} + u\frac{\partial v}{\partial x} + v\frac{\partial v}{\partial y} = -\frac{1}{\rho}\frac{\partial p}{\partial y} + \nu\left(\frac{\partial^2 v}{\partial x^2} + \frac{\partial^2 v}{\partial y^2}\right) - g[1 - \beta(T - T_0)] \tag{6.207}$$

$$\frac{\partial T}{\partial t} + u\frac{\partial T}{\partial x} + v\frac{\partial T}{\partial y} = \alpha\left(\frac{\partial^2 T}{\partial x^2} + \frac{\partial^2 T}{\partial y^2}\right) \tag{6.208}$$

Immediately after imposing of the temperature difference, the fluid is still motionless, hence the energy equation (6.208) reflects the balance between the thermal inertia and the conduction in the fluid. The scales of the two terms enclosed in the parentheses on the right-hand side of eq. (6.208) are $\Delta T / \delta_t^2$ and $\Delta T / H^2$, respectively. Since , $\delta_t \ll H$ one can conclude that $\partial^2 T / \partial y^2 \ll \partial^2 T / \partial x^2$. The balance of scales for eq. (6.208) then becomes:

$$\frac{\Delta T}{t} \sim \alpha \frac{\Delta T}{\delta_t^2}$$

Thus, the scale of the thermal boundary layer thickness becomes:

$$\delta_T \sim (\alpha t)^{1/2} \qquad (6.209)$$

To estimate the scale of the velocity, one can combine eqs. (6.206) and (6.207) by eliminating the pressure to obtain:

$$\frac{\partial}{\partial x}\left(\frac{\partial v}{\partial t}+u\frac{\partial v}{\partial x}+v\frac{\partial v}{\partial y}\right)-\frac{\partial}{\partial y}\left(\frac{\partial u}{\partial t}+u\frac{\partial u}{\partial x}+v\frac{\partial u}{\partial y}\right)$$

$$=\nu\left[\frac{\partial}{\partial x}\left(\frac{\partial^2 v}{\partial x^2}+\frac{\partial^2 v}{\partial y^2}\right)-\frac{\partial}{\partial y}\left(\frac{\partial^2 u}{\partial x^2}+\frac{\partial^2 u}{\partial y^2}\right)\right]+g\beta\frac{\partial T}{\partial x} \qquad (6.210)$$

where the left-hand side represents the inertia terms, and the right-hand side represents the viscosity and buoyancy terms. The scales of these three effects are shown below

Inertia	Viscosity	Buoyancy
$\frac{v}{\delta_T t}$	$\nu\frac{v}{\delta_T^3}$	$\frac{g\beta\Delta T}{\delta_T}$

(6.211)

To examine the relative strength of each effect, one can divide the above expression by the scale of viscosity effect to obtain

Inertia	Viscosity	Buoyancy
$\frac{1}{\mathrm{Pr}}$	1	$\frac{g\beta \Delta T \delta_T^2}{\nu v}$

where eq. (6.209) was used to simplify the inertia term. For the fluid with Pr>1, the momentum balance at requires a balance between the viscosity and buoyancy terms:

$$1 \sim \frac{g\beta \Delta T \delta_T^2}{\nu v}$$

Substituting eq. (6.209) into the above expression and rearranging the resultant expression, the scale of vertical velocity at the initiation of the natural convection is obtained as following:

$$v \sim \frac{g\beta \Delta T \alpha\, t}{v} \tag{6.212}$$

As time increases, the effect of the inertia term in eq. (7.208) weakens, hence the effect of advection becomes stronger. This trend continues until a final time, t_f, when the energy balance requires balance between the advection and conduction terms, i.e.,

$$v\frac{\Delta T}{H} \sim \alpha \frac{\Delta T}{\delta_{T,f}^2} \sim \frac{\Delta T}{t_f}$$

Thus, the scale of t_f becomes

$$t_f \sim \left(\frac{\nu H}{g\beta \Delta T \alpha} \right)^{1/2} \tag{6.213}$$

The thermal boundary layer thickness at time t_f is:

$$\delta_{T,f} \sim (\alpha t_f)^{1/2} \sim H \mathrm{Ra}_H^{-1/4} \tag{6.214}$$

At time t_f, natural convection in the rectangular enclosure reaches steady-state and the thickness of the thermal boundary layer no longer increases with time.

The wall jet thickness increases with time until $t = t_f$, when the maximum wall jet thickness, $\delta_{v,f}$, is reached (see Fig. 6.19). Outside the thermal boundary layer, the buoyancy force is absent and the thickness of the wall jet can be determined by balancing the inertia and viscosity terms in eq. (6.210):

$$\frac{v}{\delta_v t} \sim \nu \frac{v}{\delta_v^3}$$

which can be rearranged to obtain:

$$\delta_v \sim (\nu t)^{1/2} \sim \mathrm{Pr}^{1/2} \delta_T \tag{6.215}$$

For $t > t_f$, steady-state has been reached, and the wall jet thickness is related to the thermal boundary layer thickness by $\delta_{v,f} \sim \mathrm{Pr}^{1/2} \delta_{T,f}$.

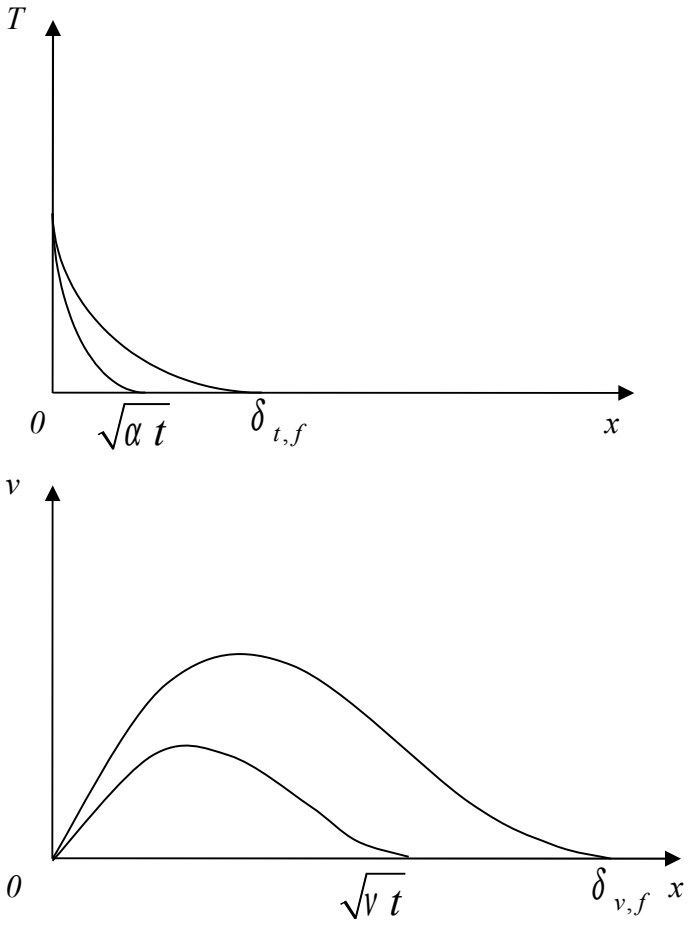

Figure 6.19 Two-layer structure near the heated wall.

Similarly, the condition to have distinct vertical wall jets or momentum boundary layers is $\delta_{v,f} < L$, or equivalently:

$$\frac{H}{L} < \mathrm{Ra}_H^{1/4}\,\mathrm{Pr}^{-1/2} \qquad (6.216)$$

When the vertical wall jet encounters the horizontal wall, it will turn to the horizontal direction and become a horizontal jet. This horizontal jet will contribute to the convective heat transfer from the heated wall to the cooled wall:

$$q'_{conv} \sim \rho\, v_f \delta_{T,f} c_p \Delta T$$

Considering eqs. (6.212) and (6.214), the above scale of convective heat transfer becomes:

$$q'_{conv} \sim k \Delta T \mathrm{Ra}_H^{1/4}$$

When a warm jet is formed at the top and a cold jet is formed at the bottom, there will be a temperature gradient along the vertical direction. The heat conduction due to this temperature gradient is:

$$q'_{cond} \sim kL\frac{\Delta T}{H}$$

The condition under which that the horizontal wall jets can maintain their temperature identity is that the heat conduction along the vertical direction is negligible compared to the energy carried by the horizontal jets:

$$kL\frac{\Delta T}{H} < k\Delta T\mathrm{Ra}_H^{1/4}$$

or equivalently

$$\frac{H}{L} > \mathrm{Ra}_H^{-1/4} \qquad (6.217)$$

The characteristics of various heat transfer regimes are summarized in Table 6.2.

Table 6.2 Characteristics of natural convection in a rectangular enclosure heated from the side

Regimes	I: Conduction	II: Tall Systems	III: Boundary layer	IV: Shallow systems
Condition of occurrence	$\mathrm{Ra}_H < 1$	$H/L > \mathrm{Ra}_H^{1/4}$	$\mathrm{Ra}_H^{-1/4} < H/L < \mathrm{Ra}_H^{1/4}$	$H/L < \mathrm{Ra}_H^{-1/4}$
Flow pattern	Clockwise circulation	Distinct boundary layer on top and bottom walls	Boundary layer on all four walls. Core remains stagnant	Two horizontal wall jets flow in opposite directions.
Effect of flow on heat transfer	Insignificant	Insignificant	Significant	Significant
Heat transfer mechanism	Conduction in horizontal direction	Conduction in horizontal direction	Boundary layer convection	Conduction in vertical direction
Heat transfer	$q' \sim kH\Delta T/L$	$q' \sim kH\Delta T/L$	$q' \sim (k/\delta_{T,f})H\Delta T$	$q' \sim (k/\delta_{T,f})H\Delta T$

6.5.2 Rectangular Enclosures

- **Heated from the Side**

  Heat transfer in regimes I and II, shown in Table 6.2, is dominated by conduction and the fluid circulation plays an insignificant role. Therefore, heat transfer in these two regimes is practically equal to the heat transfer rate estimated using Fourier's law. The flow pattern in regime III is of the boundary layer type and the core of the fluid is stagnant and stratified. The fluid flow and heat transfer in regime III can be obtained via boundary layer analysis.

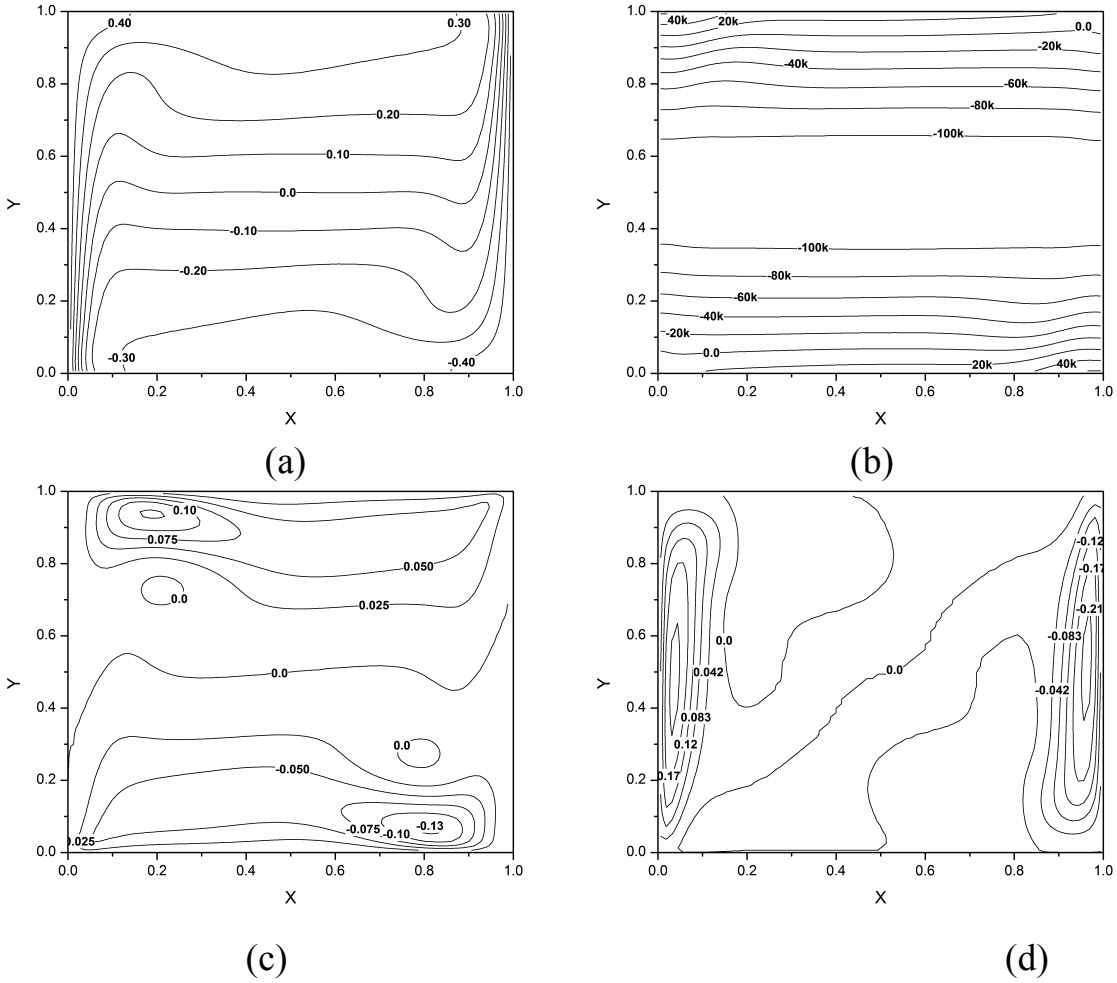

Figure 6.20 Natural convection in a square enclosure ($Ra_H = 10^6$, Pr=0.71). Steady-state distributions of dimensionless (a) temperature, (b) pressure, (c) horizontal velocity, and (d) vertical velocity (Wang *et al.*, 2010)

Figure 6.20 shows contours of dimensionless temperature, pressure, and horizontal and vertical velocities for natural convection in a square enclosure ($H/L = 1$) heated from its left side and cooled from its right side while insulated from the top and bottom. For a high Rayleigh number, the average Nusselt number for regime III, as obtained from boundary layer analysis, is

$$\overline{\mathrm{Nu}}_H = 0.364 \frac{L}{H} \mathrm{Ra}_H^{1/4} \tag{6.218}$$

which indicates that the heat transfer in the natural convection in a rectangular enclosure is dominated by both the Rayleigh number and aspect ratio.

For laminar natural convection in a rectangular enclosure with aspect ratio *H*/*L* between 1 and 10, the following correlations were suggested by Berkovsky and Polevikov:

$$\overline{\mathrm{Nu}}_H = 0.22\left(\frac{\mathrm{Pr}}{0.2+\mathrm{Pr}}\mathrm{Ra}_H\right)^{0.28}\left(\frac{L}{H}\right)^{0.09} \tag{6.219}$$

which is valid for $2 < H/L < 10,\ \mathrm{Pr} < 10^5,\ \mathrm{Ra}_H < 10^{13}$, and

$$\overline{\mathrm{Nu}}_H = 0.18\left(\frac{\mathrm{Pr}}{0.2+\mathrm{Pr}}\mathrm{Ra}_H\right)^{0.29}\left(\frac{L}{H}\right)^{-0.13} \tag{6.220}$$

which is valid for $1 < H/L < 2,\ 10^{-3} < \mathrm{Pr} < 10^5,\ 10^3 < [\mathrm{Pr}/(0.2+\mathrm{Pr})]\mathrm{Ra}_H(L/H)^3$.

For a rectangular enclosure with a larger aspect ratio, MacGregor and Emery (1969) recommended the following correlations:

$$\mathrm{Nu}_L = 0.42\mathrm{Ra}_L^{1/4}\,\mathrm{Pr}^{0.012}\left(\frac{H}{L}\right)^{-0.3} \tag{6.221}$$

which is valid for $10 < H/L < 40,\ 1 < \mathrm{Pr} < 2 \times 10^4,\ 10^4 < \mathrm{Ra}_L < 10^7$, and

$$\overline{\mathrm{Nu}}_L = 0.046\mathrm{Ra}_L^{1/3} \tag{6.222}$$

which is valid for $1 < H/L < 40,\ 1 < \mathrm{Pr} < 20,\ 10^6 < \mathrm{Ra}_L < 10^9$. It should be pointed out that the characteristic length for the Rayleigh and Nusselt numbers used in eqs. (6.221) and (6.222) is the width of the enclosure, *L*.

For the shallow enclosure represented by regime IV in Table 6.2, the horizontal wall jet flows from the left to right on the top wall and from right to the left on the bottom wall. Figure 6.21 shows streamlines and isotherms for natural convection in a shallow enclosure ($H/L = 0.1$) heated from the right side and cooled from the left side.

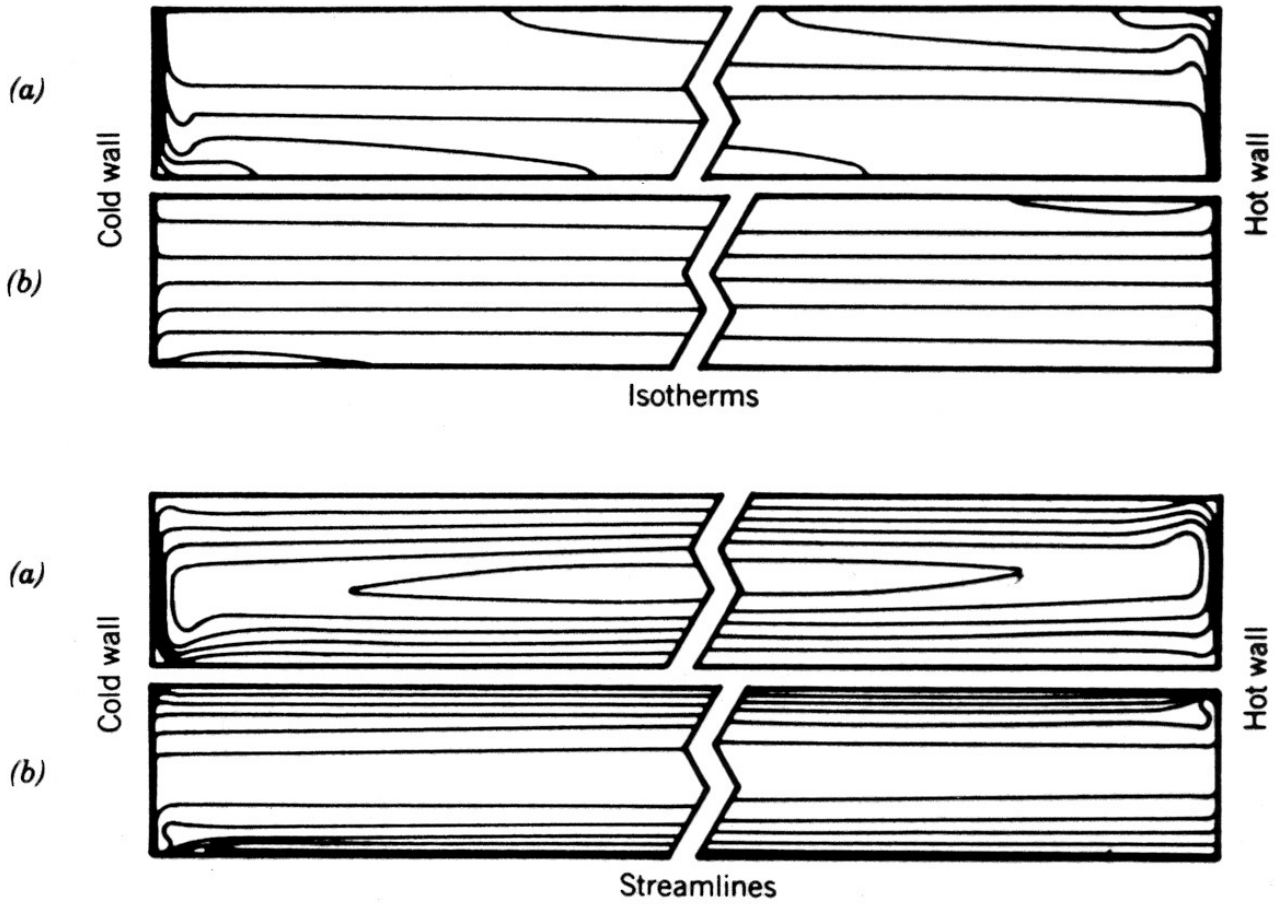

Figure 6.21 Natural convection in a shallow enclosure: (a) $Ra_H = 10^6$, (b) $Ra_H = 10^8$ ($H/L = 0.1$, Pr = 1.0; Tichy and Gadgil, 1982).

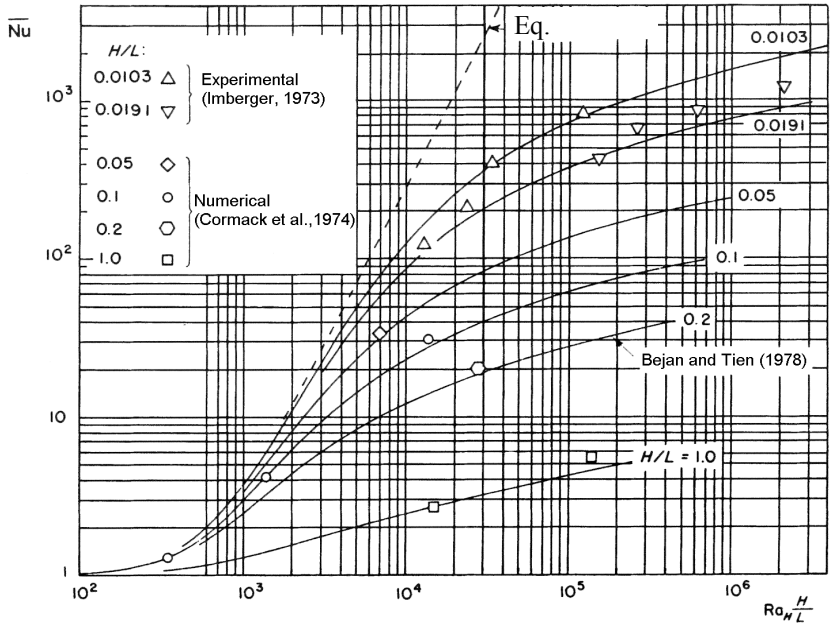

Figure 6.22 Average Nusselt number for natural convection in a shallow enclosure (Bejan and Tien, 1978).

Bejan and Tien performed a scale analysis and obtained an analytical solution via analysis of fluid flow and heat transfer in the core region. As indicated by Fig. 6.22, their results compared favorably with experimental and numerical results. For a limited case, the asymptotic heat transfer results can be expressed as:

$$\overline{\mathrm{Nu}}_H = 1 + \frac{1}{362880}\left(\frac{H}{L}\mathrm{Ra}_H\right)^2 \tag{6.223}$$

which is valid when $(H/L)^2\mathrm{Ra}_H \to 0$, and is shown as dashed line in Fig. 6.22.

Heated from the Bottom

For a rectangular enclosure filled with fluid and heated from the side, natural convection will be initiated as soon as the temperature difference between the two vertical walls is established. For a rectangular enclosure heated from below, natural convection may or may not occur depending on whether the temperature difference between the top and bottom walls exceeds a critical value. The condition for the onset of natural convection can be expressed in terms of a critical Rayleigh number.

For the case that the horizontal dimension is much larger than the height of the enclosure, the criterion for the onset of natural convection is:

$$Ra_H = \frac{g\beta \Delta T H^3}{\nu \alpha} > 1708 \qquad (6.224)$$

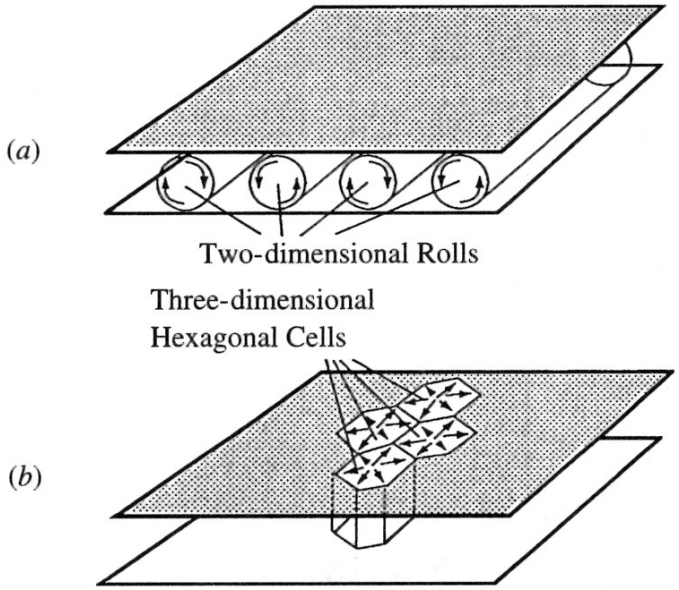

Figure 6.23 Rolls and hexagonal cells in natural convection in enclosure heated from below (Oosthuizen and Naylor, 1999).

When the Rayleigh number just exceeds the above critical Rayleigh number, the flow pattern is two-dimensional counter rotating rolls – referred to as Bénard cells [see Fig. 6.23(a)]. As the Rayleigh number further increases to one or two orders of magnitude higher than the above critical Rayleigh number, the two-dimensional cells breakup to three dimensional cells whose top view is hexagons [see Fig. 6.23(b)]. The function of the two-dimensional rolls and three-dimensional hexagonal cells is to promote heat transfer from the heated bottom wall to the cooled top wall. Globe and Dropkin suggested the following empirical correlation

$$\overline{\mathrm{Nu}}_H = 0.069 \mathrm{Ra}_H^{1/3} \mathrm{Pr}^{0.074} \qquad (6.225)$$

where all thermophysical properties are evaluated at $(T_H + T_c)/2$

Equation (6.225) is valid for $3 \times 10^5 < \mathrm{Ra}_H < 7 \times 10^9$. In addition, *H*/*L* must be sufficiently large so that the effect of the sidewalls can be negligible.

Inclined Rectangular Enclosure

When the rectangular enclosure heated from the side is tilted relative to the direction of gravity, additional unstable stratification and thermal instability will affect the fluid flow and heat transfer. The variation of Nusselt number as function of tilt angle γ is qualitatively shown in Fig. 6.24.

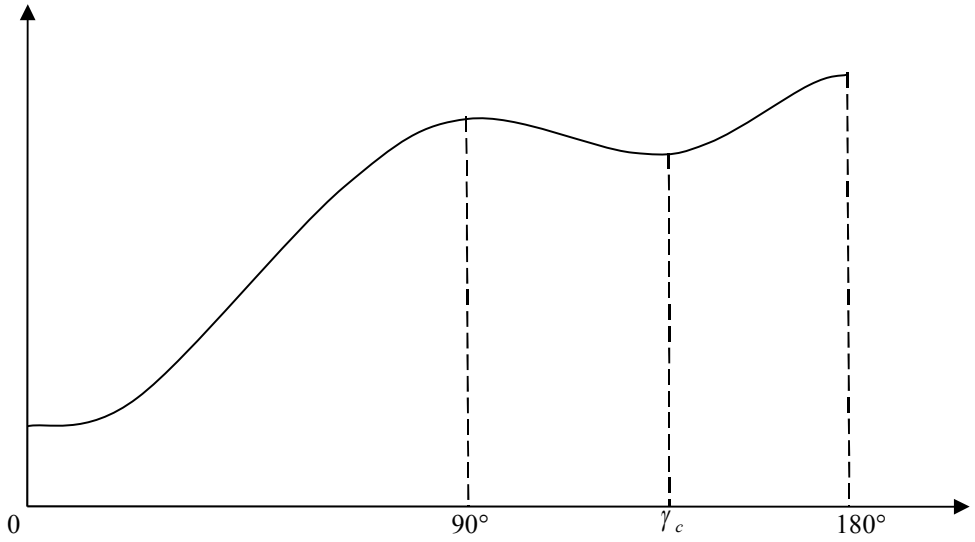

Figure 6.24 Effect of inclination angle on natural convection in enclosure

The isotherms and the streamlines for Ra=10^5 are shown in Fig. 6.25. At γ=135˚, which, according to Table 6.3, is less than the critical inclination angle, the isotherms start to exhibit some behaviors of thermally unstable conditions. This is the correlation for natural convection of air in a squared enclosure ($H/L=1$) in the region $0<\gamma<90^\circ$

$$K_\gamma = \frac{\overline{\mathrm{Nu}}_H(\gamma) - \overline{\mathrm{Nu}}_H(0^\circ)}{\overline{\mathrm{Nu}}_H(90^\circ) - \overline{\mathrm{Nu}}_H(0^\circ)} = \frac{2}{\pi}\gamma\sin\gamma \qquad (6.226)$$

where $\overline{\mathrm{Nu}}_H(0^\circ)$ is for pure conduction. While eq. (6.226) is good for air in a squared enclosure, the following correlation can be applied to other situations:

$$\frac{L}{H}\overline{\mathrm{Nu}}_H(\gamma) = \begin{cases} 1+\left[\frac{L}{H}\overline{\mathrm{Nu}}_H(90^\circ)-1\right]\sin\gamma & 0<\gamma<90^\circ \\ \frac{L}{H}\overline{\mathrm{Nu}}_H(90^\circ)(\sin\gamma) & 90^\circ<\gamma<\gamma_c \end{cases} \qquad (6.227)$$

Table 7.3 Critical inclination angle for different aspect ratio (Arnold *et al.*, 1976)

Aspect ratio, H/L	1	3	6	12	>12
Critical tilt angle, γ_c	155°	127°	120°	113°	110°

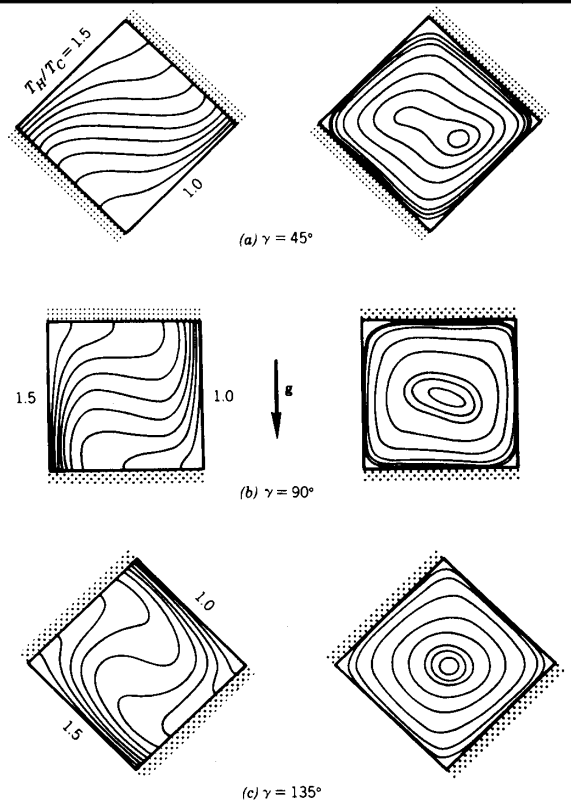

Isothermals Streamlines

Figure 6.25 Natural convection in inclined squared enclosures (Zhong *et al,* 1983).

Example 6.5

A rectangular cavity is formed by two parallel plates, each with a dimension of 0.5 m by 0.5 m, which are separated by a distance of 5 cm. The temperatures of the two plates are 37 °C and 17 °C, respectively. Find the heat transfer rate from hot plate to cold plate for the inclination angles of 0°, 45°, 90°, and 180°.

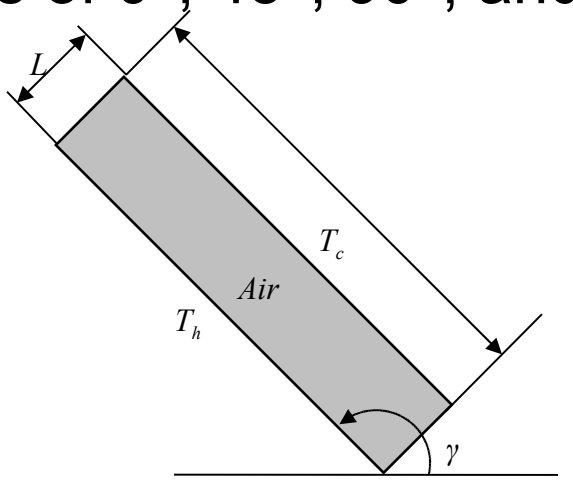

Figure 7.27 Natural convection in inclined squared enclosure.

- **Solution:**
  - $T_h = 37^\circ\text{C}$, $T_c = 17^\circ\text{C}$, $T_m = 27^\circ\text{C} = 300\text{K}$.
  - $H = 0.05$ m, $L = 0.5$ m, $D = 0.5$ m
  - From Table C.1: $\nu = 15.89 \times 10^{-6}\ \text{m}^2/\text{s}$, $k = 0.0263$ W/m-K, $\alpha = 22.5 \times 10^{-6}\ \text{m}^2/\text{s}$, and Pr = 0.707

At the inclination angle 0°, heat transfer is solely by conduction. The rate of heat transfer is

$$q(0^\circ) = kDH\frac{T_h - T_c}{L} = 0.0263 \times 0.5 \times 0.5 \times \frac{37 - 17}{0.05} = 2.63\text{W}$$

The Nusselt number for the case of pure conduction is $\overline{\mathrm{Nu}}_L(0^\circ) = 1$ or $\overline{\mathrm{Nu}}_H(0^\circ) = (H/L)\overline{\mathrm{Nu}}_L(0^\circ) = 10$. Heat transfer for the case of $\gamma = 45^\circ$ can be calculated using eq. (6.227), which requires the Nusselt number for $\gamma = 90^\circ$. Thus, the heat transfer rate for $\gamma = 90^\circ$ will be calculated first. The Rayleigh number is:

$$\mathrm{Ra}_H = \frac{g\beta\,(T_h - T_c)H^3}{\nu\,\alpha} = \frac{9.807 \times 1/300 \times (37-17) \times 0.5^3}{15.89 \times 10^{-6} \times 22.5 \times 10^{-6}} = 2.286 \times 10^8$$

The Nusselt number for $\gamma = 90^\circ$ can be obtained from eq. (6.220) :

$$\overline{\mathrm{Nu}}_H(90^\circ) = 0.18\left(\frac{\mathrm{Pr}}{0.2+\mathrm{Pr}}\mathrm{Ra}_H\right)^{0.28}\left(\frac{L}{H}\right)^{-0.13}$$

$$= 0.18 \times \left(\frac{0.707}{0.2+0.707} \times 2.286 \times 10^8\right)^{0.28}\left(\frac{0.05}{0.5}\right)^{-0.13} = 49.6$$

The heat transfer coefficient is:

$$h(90^\circ) = \frac{k\overline{\mathrm{Nu}}_H(90^\circ)}{H} = \frac{0.0263 \times 49.6}{0.5} = 2.61 \text{ W/m}^2\text{-K}$$

Therefore, the heat transfer rate for $\gamma = 90^\circ$ is:

$$q(90^\circ) = h(90^\circ)DH(T_h - T_c) = 2.61 \times 0.5 \times 0.5 \times (37 - 17) = 6.53 \text{ W}$$

When the inclination angle is $\gamma = 45^\circ = \pi/4$, eq. (6.227) yields:

$$\frac{L}{H}\overline{\mathrm{Nu}}_H(45^\circ) = 1 + \left[\frac{L}{H}\overline{\mathrm{Nu}}_H(90^\circ) - 1\right]\sin\gamma$$

$$= 1 + \left(\frac{0.05}{0.5} \times 49.6 - 1\right)\sin 45^\circ = 3.80$$

Thus, the Nusselt number is $\mathrm{Nu}_H(45^\circ) = 38.0$ and the corresponding heat transfer coefficient is:

$$h(45^\circ) = \frac{k\overline{\mathrm{Nu}}_H(45^\circ)}{H} = \frac{0.0263 \times 38.0}{0.5} = 2.00 \text{ W/m}^2\text{-K}$$

The heat transfer rate for $\gamma = 45^{\circ}$ is therefore:

$$q(45^{\circ}) = h(45^{\circ})DH(T_h - T_c) = 2 \times 0.5 \times 0.5 \times (37 - 17) = 5.00\,\mathrm{W}$$

When the inclination angle is $\gamma = 180^{\circ}$, the problem becomes natural convection in an enclosure heated from the below. The Rayleigh number is:

$$\mathrm{Ra}_L = \frac{g\beta (T_h - T_c)L^3}{\nu \alpha} = \frac{9.807 \times 1/300 \times (37 - 17) \times 0.05^3}{15.89 \times 10^{-6} \times 22.5 \times 10^{-6}} = 2.286 \times 10^5$$

The Nusselt number in this case can be obtained from eq. (6.225):

$$\overline{\mathrm{Nu}}_L(180^{\circ}) = 0.069\mathrm{Ra}_H^{1/3}\,\mathrm{Pr}^{0.074}$$

$$= 0.069 \times (2.286 \times 10^5)^{1/3} \times 0.707^{0.074} = 4.11$$

The heat transfer coefficient is

$$h(180^{\circ}) = \frac{k\overline{\mathrm{Nu}}_L(180^{\circ})}{L} = \frac{0.0263 \times 4.11}{0.05} = 2.16 \text{ W/m}^2\text{-K}$$

The heat transfer rate for is therefore,

$$q(180^{\circ}) = h(180^{\circ})DH(T_h - T_c) = 2.16 \times 0.5 \times 0.5 \times (37 - 17) = 10.80 \text{ W}$$

6.5.3 Annular Space between Concentric Cylinders and Spheres

Natural convection in spaces between long horizontal concentric cylinders or between spheres is very complicated. The only practical approach to analyze the problem is via numerical solution. The physical model of natural convection in annular space between concentric cylinders is show in Fig. 6.27.

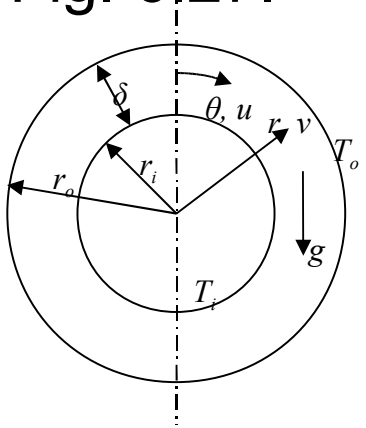

Figure 6.27 Natural convection in horizontal annular space between concentric cylinders

Since the problem is axisymmetric, one only needs to study the right half of the domain. In the coordinate system shown in Fig. 6.27, the governing equations are

$$\frac{1}{r}\frac{\partial u}{\partial \theta}+\frac{\partial v}{\partial r}+\frac{v}{r}=0 \tag{6.228}$$

$$\frac{u}{r}\frac{\partial u}{\partial \theta}+v\frac{\partial u}{\partial r}+\frac{uv}{r}=-\frac{1}{\rho r}\frac{\partial p}{\partial \theta}+\nu\left(\frac{1}{r^2}\frac{\partial^2 u}{\partial \theta^2}+\frac{1}{r}\frac{\partial u}{\partial r}+\frac{\partial^2 u}{\partial r^2}-\frac{u}{r^2}+\frac{2}{r^2}\frac{\partial v}{\partial \theta}\right) - g\beta\,(T-T_{ref})\sin\theta \tag{6.229}$$

$$\frac{u}{r}\frac{\partial v}{\partial \theta}+v\frac{\partial v}{\partial r}-\frac{u^2}{r}=-\frac{1}{\rho}\frac{\partial p}{\partial r}+\nu\left(\frac{1}{r^2}\frac{\partial^2 v}{\partial \theta^2}+\frac{1}{r}\frac{\partial v}{\partial r}+\frac{\partial^2 v}{\partial r^2}-\frac{v}{r^2}-\frac{2}{r^2}\frac{\partial u}{\partial \theta}\right) +g\beta\,(T-T_{ref})\sin\theta \tag{6.230}$$

$$\frac{u}{r}\frac{\partial T}{\partial \theta} + v\frac{\partial T}{\partial r} = \alpha\left(\frac{1}{r^2}\frac{\partial^2 T}{\partial \theta^2} + \frac{\partial^2 T}{\partial r^2} + \frac{1}{r}\frac{\partial T}{\partial r}\right) \tag{6.231}$$

where T_{ref} is a reference temperature and:

$$p_{eff} = p + \rho g\sin\theta - \rho g\cos\theta \tag{6.232}$$

is the effective pressure. Equations (6.228) – (6.231) are subject to the following boundary conditions:

$$u = 0,\ \frac{\partial v}{\partial \theta} = \frac{\partial T}{\partial \theta} = 0,\ \text{at}\ \theta = 0\ \text{or}\ \pi \tag{6.233}$$

$$u = v = 0,\ T = T_i,\ \text{at}\ r = r_i \tag{6.235}$$

$$u = v = 0,\ T = T_o,\ \text{at}\ r = r_o \tag{6.236}$$

Date (1986) solved this problem numerically using a modified SIMPLE algorithm for $\delta / D_i = 0.8$ and 0.15. Figure 6.28 shows the contours of the stream functions and isotherms at Ra = 4.7 x 10^4. The dimensionless stream function, dimensionless temperature and Rayleigh number are defined as the following

$$\Psi = \frac{\psi}{\alpha}, \quad \Theta = \frac{T - T_o}{T_i - T_o}, \quad \mathrm{Ra} = \frac{g\beta \Delta T \delta^3}{\nu \alpha} \tag{6.236}$$

Where the stream function, ψ , is defined as

$$u = -\frac{\partial \psi}{\partial r}, \quad v = \frac{1}{r}\frac{\partial \psi}{\partial \theta} \tag{6.237}$$

It can be seen that isotherms concentrate near the lower portion of the surface of the inner cylinder and the upper portion of the surface of the outer cylinder, which are indications of the development of thermal boundaries near the heated and cooled surfaces. While the contours of the streamlines have kidney-like shapes with the center of the flow rotation moves upward due to effect of natural convection.

The rate of heat transfer per unit length of the annulus can be calculated by the following correlation

$$q' \cong \frac{2.425k(T_i - T_o)}{[1+(D_i/D_o)^{3/5}]^{5/4}}\left(\frac{\mathrm{Pr}\,\mathrm{Ra}_{D_i}}{0.861+\mathrm{Pr}}\right)^{1/4} \tag{6.238}$$

Where the Rayleigh number is defined as

$$\mathrm{Ra}_{D_i} = \frac{g\beta(T_i - T_o)D_i^3}{\nu\alpha} \tag{6.239}$$

Equation (6.238) is valid for 0.7 < Pr < 6000 and Ra < 10^7. The thermophysical properties of the fluid should be evaluated at the mean temperature $(T_i + T_o)/2$. The scales of the thermal boundary layer on the inner surface of the outer cylinder and on the outer surface of the inner cylinder are:

$$\delta_o \sim D_o Ra_{D_o}^{-1/4}, \ \delta_i \sim D_i Ra_{D_i}^{-1/4}$$

It is obvious that $\delta_o > \delta_i$ since $D_o > D_i$. Equation will be valid only if the boundary layer thickness is less than the gap between the two cylinders, i.e. only if $\delta_o < D_o - D_i$. Under lower Rayleigh numbers, on the other hand, we have

$$D_o \mathrm{Ra}_{D_o}^{-1/4} > D_o - D_i \qquad (6.240)$$

and the heat transfer mechanism between two cylinders will approach pure conduction.

Instead of using eq. (6.240) to check the validity of eq. (6.238), another method is to calculate the heat transfer rate via eq. (6.238) and pure conduction model, and the larger of the two heat transfer rate should be used.

For natural convection in the annulus between two concentric spheres, the trends for the evolution of the flow pattern and isotherms are similar to the concentric cylinder except the circulation between concentric spheres has the shape of a doughnut. The empirical correlation for the heat transfer rate is

$$q = \frac{2.325\pi\, kD_i(T_i - T_o)}{[1 + (D_i / D_o)^{7/5}]^{5/4}} \left(\frac{\mathrm{Pr}\,\mathrm{Ra}_{D_i}}{0.861 + \mathrm{Pr}} \right)^{1/4} \qquad (6.241)$$

where the definition of Rayleigh number is same as for eq. (6.239). Equation (6.241) is valid for $0.7 < \mathrm{Pr} < 4000$ and $\mathrm{Ra} < 10^4$.

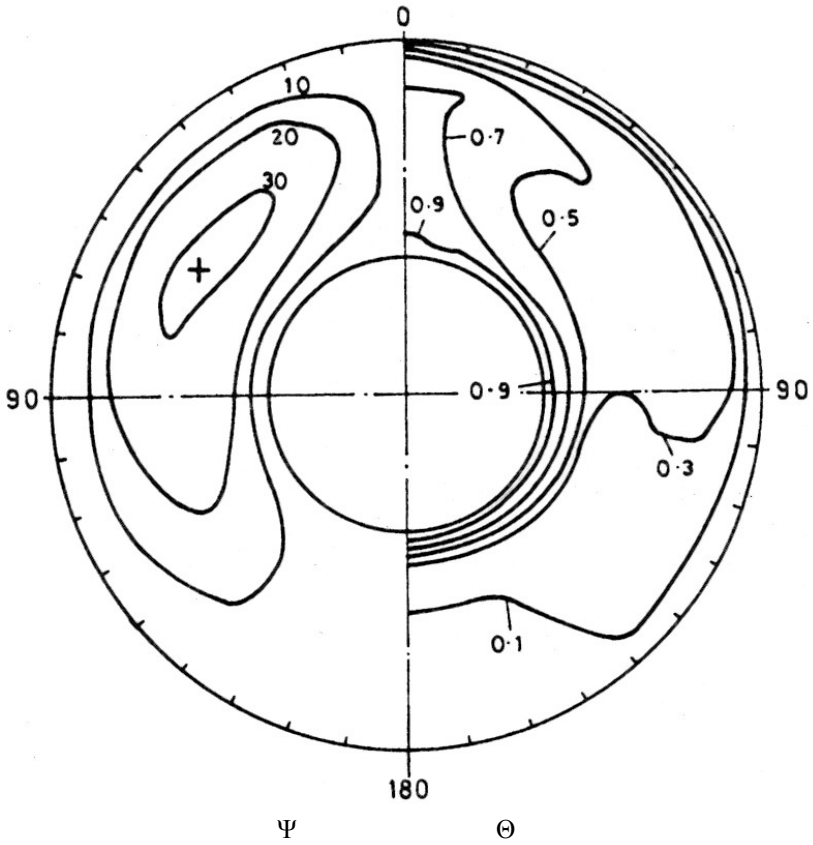

Figure 6.28 Natural convection in a horizontal annulus (Pr =0.7, δ/D_i=0.8, Ra =4.7×10^4; Date, 1986)